Diagnostic Accuracy of a MR Protocol Acquired with and without Endorectal Coil for Detection of Prostate Cancer: A Multicenter Study

Barth, Borna K ; Rupp, Niels J ; Cornelius, Alexander ; Nanz, Daniel ; Grobholz, Rainer ; Schmidtpeter, Martin ; Wild, Peter J ; Eberli, Daniel ; Donati, Olivio F

Abstract: Introduction The purpose of this study was to compare diagnostic accuracy of a prostate multiparametric magnetic resonance imaging (mpMRI) protocol for detection of prostate cancer between images acquired with and without en-dorectal coil (ERC). Materials This study was approved by the regional ethics committee. Between 2014 and 2015, 33 patients (median age 51.3 years; range 42.1-77.3 years) who underwent prostate-MRI at 3T scanners at 2 different institutions, acquired with (mpMRI) and without (mpMRI) ERC and who received radical prostatectomy, were included in this retrospective study. Two expert readers (R1, R2) attributed a PI-RADS version 2 score for the most suspect (i. e. index) lesion for mpMRI and mpMRI. Sensitivity and positive predictive value for detection of index lesions were assessed using 2 × 2 contingency tables. Differences between groups were tested using the McNemar test. Whole-mount histopathology served as reference standard. Results On a quadrant-basis cumulative sensitivity ranged between 0.61-0.67 and 0.76-0.88 for mpMRI and mpMRI protocols, respectively ($p > 0.05$). Cumulative positive predictive value ranged between 0.80-0.81 and 0.89-0.91 for mpMRI and mpMRI protocols, respectively. The differences were not statistically significant for R1 ($p = 0.267$) or R2 ($p = 0.508$). Conclusion Our results suggest that there may be no significant differences for detection of prostate cancer between images acquired with and without an ERC.

DOI: https://doi.org/10.1159/000489425

Originally published at:
Barth, Borna K; Rupp, Niels J; Cornelius, Alexander; Nanz, Daniel; Grobholz, Rainer; Schmidtpeter, Martin; Wild, Peter J; Eberli, Daniel; Donati, Olivio F (2019). Diagnostic Accuracy of a MR Protocol Acquired with and without Endorectal Coil for Detection of Prostate Cancer: A Multicenter Study. Current Urology, 12(2):88-96.
DOI: https://doi.org/10.1159/000489425

Original Paper

Current Urology

Curr Urol 2018;12:88–96
DOI: 10.1159/000489425

Received: February 1, 2018
Accepted: May 29, 2018
Published online: March 8, 2019

Diagnostic Accuracy of a MR Protocol Acquired with and without Endorectal Coil for Detection of Prostate Cancer: A Multicenter Study

Borna K. Barth[a*] Niels J. Rupp[b*] Alexander Cornelius[c] Daniel Nanz[a,d] Rainer Grobholz[e] Martin Schmidtpeter[g,f] Peter J. Wild[b,h] Daniel Eberli[i] Olivio F. Donati[a]

[a]Institute of Diagnostic and Interventional Radiology, [b]Department of Pathology and Molecular Pathology, [i]Department of Urology, University Hospital Zurich and University of Zurich, Zurich; [c]Department of Radiology, [e]Institute for Pathology, and [g]Department of Urology, Cantonal Hospital Aarau, Aarau; [d]Swiss Center for Musculoskeletal Imaging, Balgrist Campus AG, Zurich; [f]Urologiepraxis Lenzburg, Lenzburg, Switzerland; [h]Dr. Senckenberg Institute of Pathology, University Hospital Frankfurt, Frankfurt am Main, Germany

[*]These authors contributed equally, and hence share the first authorship.

Key Words
Prostate cancer • Index lesion • Endorectal coil • Diagnostic accuracy • Prostate MRI

Abstract
Introduction: The purpose of this study was to compare diagnostic accuracy of a prostate multiparametric magnetic resonance imaging (mpMRI) protocol for detection of prostate cancer between images acquired with and without endorectal coil (ERC). ***Materials:*** This study was approved by the regional ethics committee. Between 2014 and 2015, 33 patients (median age 51.3 years; range 42.1–77.3 years) who underwent prostate-MRI at 3T scanners at 2 different institutions, acquired with ($mpMRI_{ERC}$) and without ($mpMRI_{PPA}$) ERC and who received radical prostatectomy, were included in this retrospective study. Two expert readers (R1, R2) attributed a PI-RADS version 2 score for the most suspect (i.e. index) lesion for $mpMRI_{PPA}$ and $mpMRI_{ERC}$. Sensitivity and positive predictive value for detection of index lesions were assessed using 2 × 2 contingency tables. Differences between groups were tested using the McNemar test. Whole-mount histopathology served as reference standard. ***Results:*** On a quadrant-basis cumulative sensitivity ranged between 0.61–0.67 and 0.76–0.88 for $mpMRI_{PPA}$ and $mpMRI_{ERC}$ protocols, respectively ($p > 0.05$). Cumulative positive predictive value ranged between 0.80–0.81 and 0.89–0.91 for $mpMRI_{PPA}$ and $mpMRI_{ERC}$ protocols, respectively. The differences were not statistically significant for R1 ($p = 0.267$) or R2 ($p = 0.508$). ***Conclusion:*** Our results suggest that there may be no significant differences for detection of prostate cancer between images acquired with and without an ERC.

Introduction

While biopsy is still the gold standard for establishing the diagnosis of prostate cancer, multiparametric magnetic resonance imaging (mpMRI) has become an indispensable test in the diagnostic pathway of patients with suspected prostate cancer. It plays an important role within the setting of cancer detection [1], tumor localization [2, 3] and assessment of cancer aggressiveness

KARGER
Fax +41 61 306 12 34
E-Mail karger@karger.com
www.karger.com

Olivio F. Donati
Institute of Diagnostic and Interventional Radiology
University Hospital Zürich
Rämistrasse 100
CH–8091 Zurich (Switzerland)
E-Mail olivio.donati@usz.ch

Table 1. Patient demographics and histopathology data

Demographic parameter	Value
Age, year*	51.3 (42.1–77.3)
PSA at time of MRI imaging (µg/l)*	5.7 (0.3–46.0)
Time interval between mpMRI and histopathology, day*	85.5 (8–175)
Prostatectomy specimen with extracapsular extension**	11/33 (33.3)
Prostatectomy specimen with seminal vesicle infiltration**	7/33 (21.2)
Prostatectomy specimen surgical margins**	
R0	18/33 (54.6)
R1	15/33 (45.4)
Pathological stage**	
2a	2/33 (6.1)
2b	1/33 (3.0)
2c	13/33 (39.4)
3a	10/33 (30.3)
3b	7/33 (21.2)
Prevalence of index Gleason scores on histopathology**	
3 + 3	1/33 (3.0)
3 + 4	14/33 (42.4)
4 + 3	11/33 (33.3)
4 + 4	3/33 (9.1)
4 + 5	3/33 (9.1)
5 + 3	1/33 (3.0)

Thirty-three patients are in the dataset. *Data are means; data in squared parentheses are ranges. **Data are absolute counts; data in parentheses are percentages.

[4, 5]. In order to contribute valuable information for patient management, however, mpMRI must be performed and interpreted following high quality standards [6, 7]. Appropriate image quality is indispensable when interpreting mpMRI in order to establish a correct diagnosis of prostate cancer. Recommendations on minimal requirements on MRI soft- and hardware have been published [8], however no explicit recommendation is given regarding receiver coil setup. While an endorectal coil (ERC) may be particularly valuable for sequences with inherently lower signal-to-noise ratio (SNR), increased costs, artifacts and patient acceptance remain limiting factors. The ERC was shown to be useful with 1.5T scanners, where the increase in SNR directly translated into an improvement in diagnostic performance [9]. For 3T scanners and pelvic phased array (PPA) receiver coil equipment, the situation is not as clear. While it has been shown that using comparable sequence parameters, similar image quality for ERC and surface receiver coil (SRC) may be achieved [10], other studies [11–13] have demonstrated similar diagnostic accuracy with both coil settings despite lower image quality achieved with the SRC configuration. These studies however, did not investigate the diagnostic performance of a complete mpMRI protocol consisting of T2-weighted (T2w), diffusion-weighted imaging (DWI) and dynamic contrast enhanced (DCE) images and did not use whole-mount histopathology as the standard of reference. Another study has shown superior diagnostic accuracy in the detection of prostate cancer using an ERC configuration as compared to a SRC configuration [14], however the sequence parameters for the two coil configurations were not normalized in this setting. Given the equivocal results of single center studies on this topic, further investigations on receiver coil configuration are needed using comparable and optimized imaging protocols for both configurations with whole-mount histopathology as the standard of reference.

Therefore, the purpose of this multicenter study was to assess the diagnostic accuracy for prostate cancer detection between MRI protocols acquired with and without an ERC using similar sequence parameters.

Materials and Methods

The regional ethics committees approved this multicenter study, which was designed as a part of a wider cancer research project at our institution and written informed consent was obtained from all patients prior to the examination. The study was compliant with the Health Insurance Portability and Accountability Act.

Study Population

Consecutive patients undergoing mpMRI of the prostate at 3T (Tesla) acquired with two receiver coil setups, i. e. a combination of an endorectal and a PPA receiver coil ($mpMRI_{ERC}$), and a PPA receiver coil only ($mpMRI_{PPA}$), followed by a radical prostatectomy were retrospectively included into the study (n = 38; median age 67.8 years; range 51.3–77.3 years). The exams were performed within a clinical setting for either detection and/or local staging of prostate cancer between December 2014 and August 2015 at two radiology departments. Clinical indications were elevated prostate specific antigen (PSA) (median PSA 5.8 µg/l, range 0.3–46.0 µg/l) or suspicion of prostate cancer on digital rectal examination. We excluded patients with an incomplete histopathology report (n = 5). The final study population comprised of 33 patients (median age 51.3 years, range 42.1–77.3 years). Three of these patients previously had been included in a study comparing diagnostic accuracy of a standard versus shortened multiparametric MRI protocol [29], and 13 patients were previously included in a study comparing image quality of images with and without ERC [10]. Patient demographics and a summary of histopathology data is shown in table 1.

MRI Equipment

Images were acquired on a 3T whole body MRI system (MAGNETOM Skyra, Siemens Healthcare®, Erlangen, Germany) in both radiologic departments. First, the $mpMRI_{ERC}$ image set

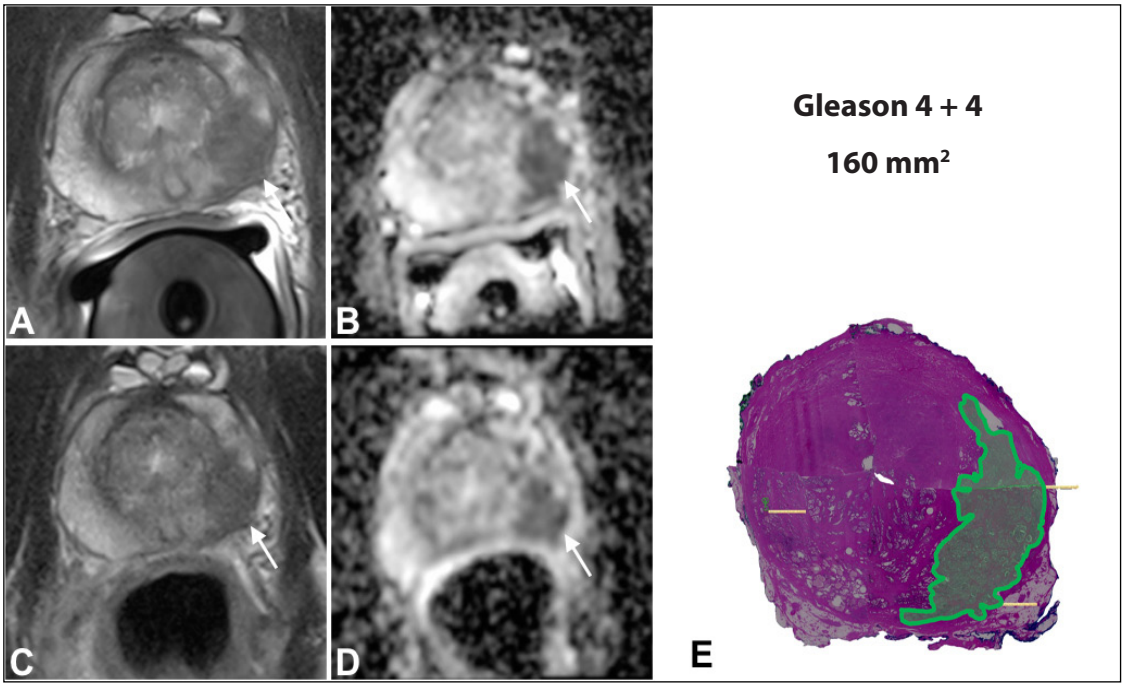

Fig. 1. A 67-year-old patient (PSA, 30 ng/ml) undergoing mpMRI of the prostate for cancer detection and local staging. T2w (**A, C**) and ADC maps (**B, D**) were used side-by-side with histopathology for correlation of every mismatched lesion. Reconstructed whole-mount histopathology (**E**) reveals a 4 + 4 tumor (approximately 160 mm^2) on the left aspect of the peripheral zone, at the level of the midgland (**E**, green ROI). At one of the two institutions the slices were digitalized and the lesions outlined electronically. T2w images with corresponding ADC maps from the $mpMRI_{ERC}$ (**A, B**) and $mpMRI_{PPA}$ (**C, D**) sets and a whole-mount histopathology (**E**) from the midgland are shown. The corresponding PI-RADS reader score was 4 for both readers and for both image sets.

was acquired using an 18-channel PPA receiver coil (Body 18, Siemens Healthcare®, Erlangen, Germany) in conjunction with a balloon-covered, expandable ERC (Medrad, Warrendale, Pa) filled with barium suspension. Secondly, the ERC was removed and images for the $mpMRI_{PPA}$ image set were acquired using the PPA receiver coil only.

Scan Parameters

T2w turbo-spin echo images were acquired in three orthogonal planes (axial, sagittal and coronal), covering the prostate gland and the seminal vesicles. DWI and echo-planar images were acquired with identical orientation as the axial T2w, and utilizing selective-excitation technology (ZOOMIt, Siemens Healthcare, Erlangen, Germany). Apparent diffusion coefficient (ADC) maps were calculated using a mono-exponential fit based on the three obtained b-values (either 0, 50, 1,000 s/mm^2). A high-b-value (1,400 s/mm^2) was calculated based upon a standard mono-exponential fit. T1w turbo-spin echo images were acquired in axial plane, using a field-of-view encompassing the whole pelvis. DCE-MRI were obtained in axial plane with a temporal resolution of < 8 seconds. Gadoterate meglumine (Dotarem; Guerbet, Darmstadt, Germany) was used as contrast agent with a dose of 0.1 mmol/kg bodyweight. Injection was performed with an automated MR injection system (Spectris Solaris EP, MEDRAD MR Injector, Bayer HealthCare LCC, Whippany NJ) at a flow rate of 2 ml/s. Sequence parameters were kept within ranges of published technical MRI guidelines [8]. Coronal and sagittal T2w images and transverse T1w turbo-spin echo images were additionally obtained during the clinical protocol but were not used for study purposes. Sequence parameters are shown in table 2.

Image Readout

Study images were de-identified. Blinding of the 2 image sets regarding to whether the images were acquired with or without the ERC was not possible. Two radiologists (reader 1 and 2) specialized in urogenital imaging (O. F. D. with 4 years and A. C. with 10 years of experience in interpreting prostate MRI) from different radiologic departments independently reviewed $mpMRI_{ERC}$ and $mpMRI_{PPA}$ image sets randomly in 2 separate reading sessions (time interval between the sessions > 4 weeks). DCE-MRI images were acquired with ERC only, and were presented in both reading sessions. The readers were aware that patients received radical prostatectomy, but were blinded to the remaining clinical information. The readers were instructed to assess the visually most suspicious lesion (hereafter termed "index lesion") according to the prostate imaging reporting and data system (PI-RADS) version

Table 2. Sequence parameters for images acquired with $mpMRI_{PPA}$ and $mpMRI_{ERC}$

	$mpMRI_{PPA}$		$mpMRI_{ERC}$		Both
	T2w	DWI	T2w	DWI	DCE-MRI
b-value, s/mm²	–	100, 600, 1000	–	100, 600, 1000	–
Number of averages	4	2, 6, 12	3	2, 4, 8	–
Typical TR, ms	3,500	5,000	3,580	5,000	5.4
Minimum TE, ms	93	75	97	96	1.8
Echo train length	25	–	25	–	–
Acquisition matrix	256 × 256	100 × 52	320 × 320	112 × 58	
In-plane resolution, mm	0.27 × 0.27	0.7 × 0.7	0.22 × 0.22	0.63 × 0.63	1 0.6
Field of view, mm²	140 × 140	140 × 73	140 × 140	140 × 73	
Slice thickness, mm	3	3	3	3	3
Pixel bandwidth, Hz/px	200	1,280	200	1,275	
Acquisition time, min:s	4:49	5:05	4:48	3:35	06:30

Table 3. PI-RADS scores attributed to the corresponding epicenter quadrants for images acquired with $mpMRI_{PPA}$ and $mpMRI_{ERC}$

PI-RADS scores	Reader 1*		Reader 2*	
	$mpMRI_{PPA}$	$mpMRI_{ERC}$	$mpMRI_{PPA}$	$mpMRI_{ERC}$
1	0 (0)	1 (3.0)	11 (33.3)	5 (15.2)
2	6 (18.2)	3 (9.1)	0 (0)	0 (0)
3	4 (12.1)	0 (0)	2 (6.1)	3 (9.1)
4	12 (36.4)	17 (51.5)	9 (27.3)	15 (45.5)
5	11 (33.3)	12 (36.4)	11 (33.3)	10 (30.3)

Thirty-three patients are in the dataset. *Data are absolute counts; data in parentheses are percentages.

2 criteria [15] for each patient. Both readers had previously used the PI-RADS within their clinical routine and thus were familiar with it. The index lesion was attributed to one of the eight equal prostate sectors (anterior right, posterior right, anterior left and posterior left; four each within the apex and the base of the gland), which was a modification of the 36-sector map proposed by PI-RADS version 2 [15]. Lesions involving more than 1 sector were attributed to the predominantly involved sector.

The readout was performed using an electronic reader form and patient data was stored on a secured mobile hard drive at our institution.

Reference Standard

Histopathology was performed by experienced genitourinary pathologists (N.J.R. with 5 and R.G with 20 years of experience in interpreting prostatectomies). Each prostate specimen was formalin fixed, processed and embedded in paraffin in axial orientation and perpendicularly to the urethra. Five millimeter (mm) thick tissue blocks were made from the apex to the base, labelled sequentially and stained with hematoxylin-eosin for histopathological evaluation. Morphological grading was performed according to the standards of the ISUP Gleason Grading of Prostatic Carcinoma [16]. Gleason score (GS), topographic location and the maximal diameter were assigned to the lesion with the highest GS, or if 2 or more equally scored lesions were present, the one with the largest diameter (i. e. index lesion). Pathological staging was performed according to the 8th edition of the Union for International Cancer Control TNM classification of malignant tumours [17]. In one of the 2 institutions the slices were digitalized, whole slides reconstructed and all lesions, including the index lesion, were outlined electronically including information about exact area and GS (fig. 1). In the other institution, the lesions were manually mapped on a standardized template sheet, which subdivided the prostate into 16 sectors (i. e. 4 quadrants within the apex, apex-to-midgland, midgland-to-base and base, respectively).

Post-processing of Readout and Histopathology Data

A third radiologist (B. K. B. 3 years of experience in interpreting prostate MRI) not involved in the readout performed the post-processing. First, the PI-RADS scores from corresponding sectors from the base and the apex were aggregated to 4 quadrants (base left/right; apex left/right) by assigning the highest reader score for each quadrant. For side-based analysis the scores were further aggregated by assigning the highest score from quadrant-based analysis to each corresponding side and for patient-based analysis, the reader scores were aggregated by assigning the highest reader score to each patient. The scores were dichotomized by considering 1–3 as negative, and 4–5 as positive. Second, the 16 sectors from the standardized template sheets were summarized into quadrants, consequently attributing the index lesion

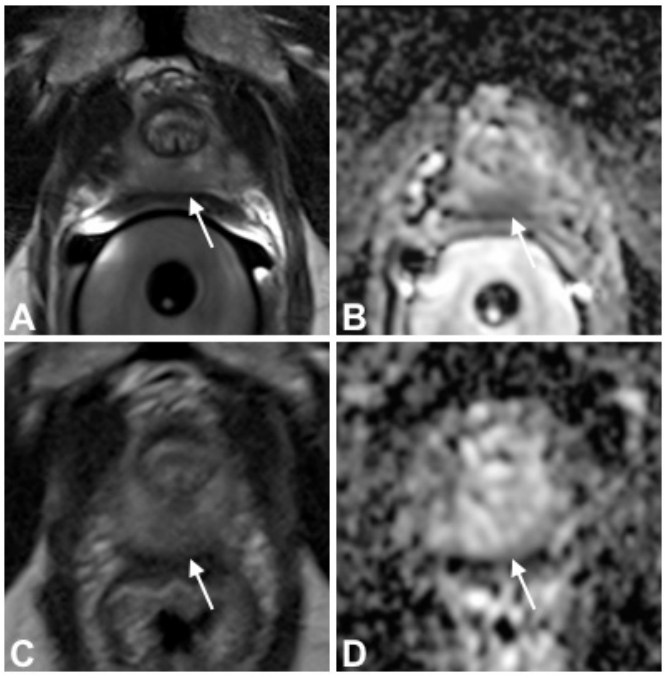

Fig. 2. A 54-year-old patient (PSA, 7.7 ng/ml) undergoing mpMRI of the prostate for detection and local staging. On the $mpMRI_{ERC}$ image set, the tumor (arrow) is clearly appreciated on the posterior median aspect of the apex, showing focal T2w hypointensity (**A**) and corresponding diffusion restriction on the ADC-map (**B**). On the $mpMRI_{PPA}$ image set however, the tumor is less evident on T2w series (**C**) and does show no clearly appreciable diffusion restriction on the ADC map (**D**). Both readers only identified the tumor using the $mpMRI_{ERC}$ image set (**A, B**).

to the predominantly involved quadrant [i. e. epicenter quadrant (EC_Q)] as shown before [18]. On digitalized histopathology the index lesion was directly attributed to the predominantly involved quadrant. Finally, careful side-by-side MRI-to-histopathology correlation was performed on a visual basis for every mismatch, rendering those lesions true positive on the readout, which were considered to be the same as the index lesion marked on histopathology (i. e. lesions invading more than 1 quadrant, however the quadrant not being the EC_Q) (fig. 1). A finding on MRI was rated true positive if it occurred in any of the regions comprising the index lesion as defined by the pathologist. A finding on MR was classified as false positive if its attributed region did not match the region of the index lesion as defined by the pathologist. If the region of the index lesion as defined by the pathologist was not rated as positive on MR, the MR finding was rated false negative.

Statistical Analysis

Continuous variables were summarized by using means and SD. Categorical variables were summarized as counts and proportions. Kolmogorov-Smirnov test was used to assess the distribution of data.

Sensitivity and positive predictive value (PPV) for detection of index lesions were assessed using 2 × 2 contingency tables for the dichotomized data sets. Analysis was performed on a quadrant, side, and patient-basis for the $mpMRI_{PPA}$ and $mpMRI_{ERC}$ image set. Sensitivity and PPV for quadrant and side-based analysis was cumulated to one value. Differences between groups were tested using the McNemar test. Intra- and inter-reader agreement for the dualized scores was assessed using Cohen's Kappa (κ). κ-values were stratified qualitatively by score (slight agreement 0.01–0.20; fair agreement 0.21–0.40; moderate agreement 0.41–0.60; substantial agreement 0.61–0.80; very good agreement 0.81–0.99) [19].

A p-value of < 0.05 was considered statistically significant. Statistical analysis was performed with IBM SPSS statistical software (SPSS version 21; Chicago, Ill).

Results

Patient Demographics

Thirty-three patients were included. The most prevalent GS was 3 + 4 (n = 14 patients), followed by 4 + 3 (n = 11 patients), 4 + 4 (n = 3 patients), 4 + 5 (n = 3 patients), 3 + 3 (n = 1 patient) and 5 + 3 (n = 1 patient). T-stage was < T3 for n = 16 patients ≥ T3 for n = 17 patients. Fifteen patients were stratified as "intermediate risk" and 18 patients as "high risk", according to the D'Amico risk group classification [20]. Patient demographics and histopathology data and are shown in table 1.

The frequency of PI-RADS 4 and 5 scores attributed to the corresponding epicenter quadrants was 69.7% (n = 23) for R1 and 60.6% (n = 20) for R2 for images acquired with the $mpMRI_{PPA}$. For images acquired with the $mpMRI_{ERC}$ the frequency was 87.9% (n = 29) for R1 and 75.8% (n = 25) for R2. The scores attributed to the corresponding epicenter quadrants are shown in table 3.

Diagnostic Accuracy

On a quadrant basis cumulative sensitivity for the detection of the index lesion was lower for both readers for images acquired with the $mpMRI_{PPA}$ (R1, 0.67 and R2, 0.61), compared with $mpMRI_{ERC}$ (R1, 0.88 and R2, 0.76). Cumulative PPV was lower for images acquired with the $mpMRI_{PPA}$ (R1, 0.81 and R2, 0.80), compared with $mpMRI_{ERC}$ (R1, 0.91 and R2, 0.89). The difference between the two coil setups was not statistically significant (R1, $p = 0.267$ and R2, $p = 0.508$) (fig. 2, 3). Comparable results were achieved on a side-based analysis, namely cumulative sensitivity being lower for both readers for images acquired with the $mpMRI_{PPA}$ (R1, 0.70 and R2, 0.67), compared with $mpMRI_{ERC}$ (R1, 0.91 and R2, 0.79). The same is true for the cumulative PPV for images acquired

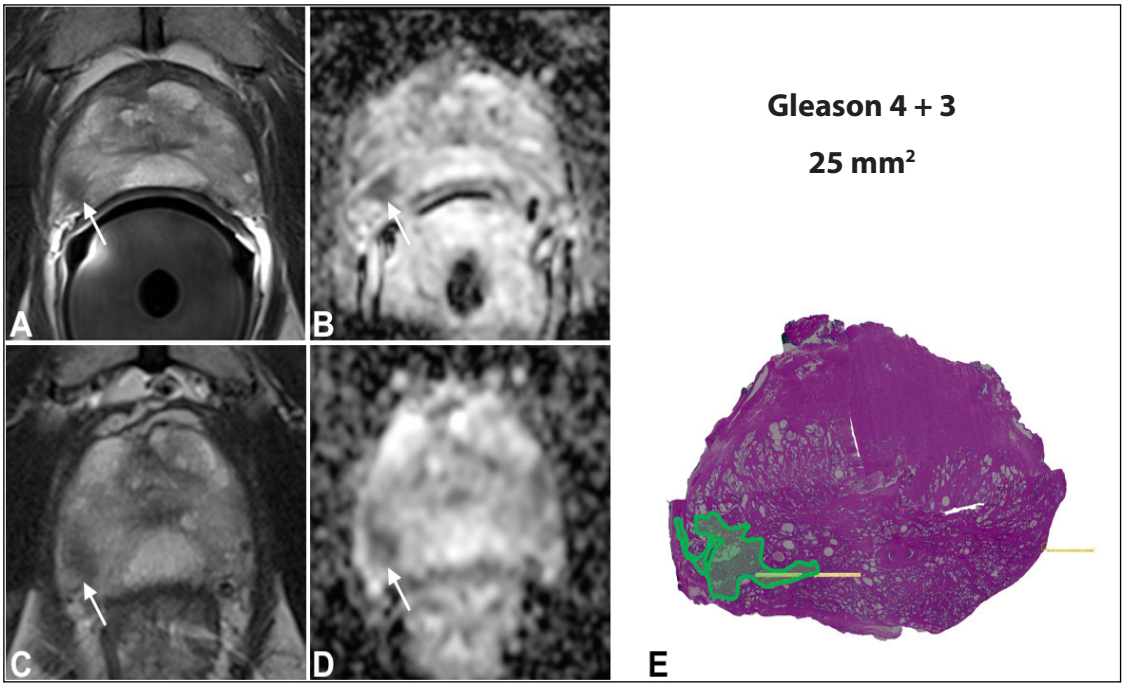

Fig. 3. A 56-year-old patient undergoing mpMRI of the prostate for local staging of a bioptically diagnosed 4 + 3 tumor on the right side of the gland. On the $mpMRI_{ERC}$ image set, the tumor (arrow) is clearly appreciated on the postero-lateral aspect of the right midgland, showing focal T2w hypointensity (**A**) and corresponding diffusion restriction on the ADC-map (**B**). The same is true for the $mpMRI_{PPA}$ image set (**C, D**). Both readers correctly identified the tumor using both image sets. Reconstructed whole-mount histopathology (**E**) reveals a 4 + 3 tumor (approximately 25 mm^2) on the postero-lateral aspect of the peripheral zone, at the level of the right midgland (**E**, green ROI). Both readers correctly identified the tumor by attributing a PI-RADS score of 4 to the corresponding quadrant, using the $mpMRI_{ERC}$ and the $mpMRI_{PPA}$ image set.

with the $mpMRI_{PPA}$ (R1, 0.85 and R2, 0.88), compared with $mpMRI_{ERC}$ (R1, 0.94 and R2, 0.93). The difference between the two coil setups, again was not statistically significant (R1, p = 0.267 and R2, p = 0.453). The same trend can be observed on a patient-basis, namely sensitivity being lower for both readers for images acquired with the $mpMRI_{PPA}$ (R1, 0.82 and R2, 0.76), compared with $mpMRI_{ERC}$ (R1, 0.97 and R2, 0.85), the difference not being statistically significant (R1, p = 0.063 and R2, p = 0.375). Results of the assessment of diagnostic accuracy are shown in table 4.

Inter- and Intra-reader Agreement

Interreader agreement across all sub-analyses was good (κ range 0.64–0.76) for $mpMRI_{PPA}$ and fair-very good (κ range 0.3–0.83) for $mpMRI_{ERC}$, respectively. Intrareader agreement across all sub-analyses was fair-good (κ range 0.25–0.72) for Reader 1 and moderate-very good (κ range 0.53–0.84) for Reader 2, respectively.

Discussion

Receiver coil equipment is an important determinant of image quality in MRI of the prostate. Due to the possibility to be placed directly in close proximity of the posterior circumference of the organ, a high SNR can be achieved by means of an ERC, however potentially at the expense of increased artifacts [21] and higher costs. Our results, demonstrating that prostate cancer foci may be detected without significantly lower sensitivity by use of a PPA receiver coil as compared to an ERC, suggest that the potentially lower SNR does not translate into a lower diagnostic performance.

Whether to use an ERC or not is a matter of intense debate in prostate imaging. Apart from investigating image quality, some authors already conducted studies comparing the diagnostic accuracy of various coil setups. For local cancer staging, the use of an ERC as compared to PPA receiver coil equipment alone seems favorable,

Table 4. Diagnostic accuracy of images sets with $mpMRI_{PPA}$ and $mpMRI_{ERC}$

PI-RADS scores	Quadrant-based			Side-based			Patient-based		
	$mpMRI_{PPA}$	$mpMRI_{ERC}$	p	$mpMRI_{PPA}$	$mpMRI_{ERC}$	p	$mpMRI_{PPA}$	$mpMRI_{ERC}$	p
Diagnostic accuracy reader 1			0.267			0.267			0.063
True positives	22	29		23	30		27	32	
False positives	5	3		4	2		N/A	N/A	
False negatives	11	4		10	3		6	1	
Sensitivity	0.67*	0.88*		0.7*	0.91*		0.82	0.97	
PPV	0.81*	0.91*		0.85*	0.94*		N/A	N/A	
Diagnostic accuracy reader 2			0.508			0.453			0.375
True positives	20	25		22	26		25	28	
False positives	5	3		3	2		N/A	N/A	
False negatives	13	8		11	7		8	5	
Sensitivity	0.61*	0.76*		0.67*	0.79*		0.76	0.85	
PPV	0.80*	0.89*		0.88*	0.93*		N/A	N/A	

Thirty-three patients are in the dataset. *Cumulative sensitivity of all quadrants and prostate halves, respectively is given.

particularly at lower field strengths [22, 23]. Therefore, the European Society of Urogenital Radiology still recommends to use the ERC for local staging of prostate cancer on a 1.5T MRI in their recently updated guidelines [15]. For detection of cancer foci, there is no clear recommendation on the choice of receiver coil setup, especially when performing MRI at higher field strengths (3T). While Turkbey et al. [14] demonstrated better sensitivity and PPV on images acquired with the ERC as compared to PPA (ERC 0.76 and 0.80; PPA 0.45 and 0.64) for all tumors, a sub-analysis of dominant tumors did not show such a distinct difference (sensitivity of ERC 0.85; sensitivity for PPA 0.75). These findings are in accordance with our results with an overall sensitivity for detection of index lesions of 0.82 (mean value of R1, R2) for the $mpMRI_{ERC}$ image set and 0.64 (mean value of R1, R2) for the $mpMRI_{PPA}$ image set, respectively. The ERC image set showed a tendency towards higher sensitivity as compared to the image set acquired with the PPA receiver coil only, however, differences were not statistically significant. Another recent study supports our findings by demonstrating insignificant differences between receiver coil setups for the detection of index lesions [11]. Our achieved sensitivities of 0.76–0.97 on a per patient basis, are lower than the achieved sensitivities in the aforementioned study (0.96–0.97). A possible explanation may be the different reference standards used in the 2 studies (MRI-TRUS fusion biopsy vs. prostatectomy specimens).

Another study [24] investigating the diagnostic performance of images acquired without an ERC found that index lesions can be detected with an average sensitivity and PPV of 60.2 and 65.3%, respectively. When correcting for a mismatch in terms of localization, similarly to the matching procedure used in our study, the overall performance rose to 75.9 and 82.6%, which is comparable with our results (sensitivity average R1, R2 for both coil combinations, 0.73 and PPV, 0.85). The difference in sensitivity between the two receiver coil combinations in our study on a patient basis translated to n = 5 and 3 patients for R1 and R2, respectively which were missed. The reason for the false negatives may be rooted in the reduced SNR provided by the PPA coil setup. This decrease in SNR may be minimized by increasing the number of averages for PPA acquisition, a solution that will be entailed by an increase in acquisition time, however.

To reliably detect prostate cancer is one of the major tasks of mpMRI. Its ability in doing so varies significantly in the literature [25–28] and rises up to > 90% when assessed on a patient basis (sensitivity range 79–96%) [29–33]. These results are comparable with our study, where sensitivity ranged between 0.85 and 0.97 with and 0.76 and 0.82 without the usage of an ERC, and demonstrate that images acquired without an ERC may be sufficient for the purpose of detection of prostate cancer. Inter- and intra-reader agreement in our study was within the range of previously published results [34–37] and did not differ between the two coil setups investigated.

Several limiting factors are associated with the use of an ERC, more precisely patient acceptance, increased costs and associated artifacts. Therefore, further efforts must be undertaken in order to optimize MRI sequences up to a level where image quality does not compromise diagnostic performance. We think that with additional

scan time, which would otherwise be used for other procedural steps, like coil insertion and patient preparation, image quality could be improved, potentially closing the gap of false negative lesions which we observed in our analysis.

Our study has limitations. First, we were unable to analyze all tumor lesions present in the prostate gland, as histopathologic data from one of the two institutions did not allow for clear labeling of the tumor foci with respect to Gleason grade and size, except for the index lesion. While it usually is the index lesion which is determinant for the therapeutic strategy and management of the patient, non-inclusion of all but the index lesions into our analysis did not allow for assessment of "true negative" prostate quadrants and therefore the specificity and the negative predictive value could not be evaluated. Second, a discrimination between tumors in the transitional and the peripheral zone was not possible. However, in clinical practice, accurate topographic localization of the lesion is of more importance, than the ability to attribute a certain finding to a specific intraprostatic region. Third, the relatively small patient population may have prevented the detection of a statistically significant difference between the coil setups. Therefore further, preferably multicenter studies, will be necessary in order to provide clearer suggestions on the optimal coil setup for prostate cancer detection. Blinding of the readers regarding the utilized coil setup or regarding to the fact that all patients received radical prostatectomy was not possible which may have introduced interpretation and selection bias. Blinding of the coil setup was impossible, as even with cropped images, parts of the ERC will always be visible on the images to analyze. Finally, using DCE-MRI sequences, acquired with the ERC in conjunction with the $mpMRI_{PPA}$ images represents a bias. However, due to ethical reasons we abstained from administering contrast media twice within one exam. As DCE-MRI represents an integral component of PI-RADS version 2, we did not exclude this sequence.

In conclusion, our results suggest that there may be no significant differences for detection of prostate cancer between images acquired with an ERC and those acquired with a PPA coil.

References

1 Scheenen TW, Rosenkrantz AB, Haider MA, Futterer JJ: Multiparametric magnetic resonance imaging in prostate cancer management: current status and future perspectives. Invest Radiol 2015;50:594–600.

2 Rosenkrantz AB, Shanbhogue AK, Wang A, Kong MX, Babb JS, Taneja SS: Length of capsular contact for diagnosing extraprostatic extension on prostate MRI: assessment at an optimal threshold. J Magn Reson Imaging 2016;43:990–997.

3 Rosenkrantz AB, Triolo MJ, Melamed J, Rusinek H, Taneja SS, Deng FM: Whole-lesion apparent diffusion coefficient metrics as a marker of percentage Gleason 4 component within Gleason 7 prostate cancer at radical prostatectomy. J Magn Reson Imaging 2015;41:708–714.

4 Donati OF, Afaq A, Vargas HA, Mazaheri Y, Zheng J, Moskowitz CS, Hricak H, Akin O: Prostate MRI: evaluating tumor volume and apparent diffusion coefficient as surrogate biomarkers for predicting tumor Gleason score. Clin Cancer Res 2014;20:3705–3711.

5 Donati OF, Mazaheri Y, Afaq A, Vargas HA, Zheng J, Moskowitz CS, Hricak H, Akin O: Prostate cancer aggressiveness: assessment with whole-lesion histogram analysis of the apparent diffusion coefficient. Radiology 2014;271:143–152.

6 Starobinets O, Korn N, Iqbal S, Noworolski SM, Zagoria R, Kurhanewicz J, Westphalen AC: Practical aspects of prostate MRI: hardware and software considerations, protocols, and patient preparation. Abdom Radiol (NY) 2016;41:817–830.

7 Qayyum T, Willder JM, McArdle PA, Horgan PG, Edwards J, Underwood MA: The accuracy of magnetic resonance imaging in radical prostatectomy. Curr Urol 2013;7:62–64.

8 Barentsz JO, Richenberg J, Clements R, Choyke P, Verma S, Villeirs G, Rouviere O, Logager V, Futterer JJ: ESUR prostate MR guidelines 2012. Eur Radiol 2012;22:746–757.

9 Torricelli P, Cinquantini F, Ligabue G, Bianchi G, Sighinolfi P, Romagnoli R: Comparative evaluation between external phased array coil at 3 T and endorectal coil at 1.5 T: preliminary results. J Comput Assist Tomogr 2006;30:355–361.

10 Barth BK, Cornelius A, Nanz D, Eberli D, Donati OF: Comparison of image quality and patient discomfort in prostate MRI: pelvic phased array coil vs. endorectal coil. Abdom Radiol (NY) 2016;41:2218–2226.

11 Baur AD, Daqqaq T, Wagner M, Maxeiner A, Huppertz A, Renz D, Hamm B, Fischer T, Durmus T: T2- and diffusion-weighted magnetic resonance imaging at 3T for the detection of prostate cancer with and without endorectal coil: An intraindividual comparison of image quality and diagnostic performance. Eur J Radiol 2016;85:1075–1084.
12 Gawlitza J, Reiss-Zimmermann M, Thormer G, Schaudinn A, Linder N, Garnov N, Horn LC, Minh DH, Ganzer R, Stolzenburg JU, Kahn T, Moche M, Busse H: Impact of the use of an endorectal coil for 3 T prostate MRI on image quality and cancer detection rate. Sci Rep 2017;7:40640.
13 Ullrich T, Quentin M, Oelers C, Dietzel F, Sawicki LM, Arsov C, Rabenalt R, Albers P, Antoch G, Blondin D, Wittsack HJ, Schimmoller L: Magnetic resonance imaging of the prostate at 1.5 versus 3.0T: a prospective comparison study of image quality. Eur J Radiol 2017;90:192–197.
14 Turkbey B, Merino MJ, Gallardo EC, Shah V, Aras O, Bernardo M, Mena E, Daar D, Rastinehad AR, Linehan WM, Wood BJ, Pinto PA, Choyke PL: Comparison of endorectal coil and nonendorectal coil T2W and diffusion-weighted MRI at 3 Tesla for localizing prostate cancer: correlation with whole-mount histopathology. J Magn Reson Imaging 2014;39:1443–1448.
15 Weinreb JC, Barentsz JO, Choyke PL, Cornud F, Haider MA, Macura KJ, Margolis D, Schnall MD, Shtern F, Tempany CM, Thoeny HC, Verma S : PI-RADS prostate imaging-reporting and data system: 2015,Version 2. Eur Urol 2016;69:16–40.
16 Epstein JI, Egevad L, Amin MB, Delahunt B, Srigley JR, Humphrey PA: The 2014 International Society of Urological Pathology (ISUP) Consensus Conference on Gleason grading of prostatic carcinoma: definition of grading patterns and proposal for a new grading system. Am J Surg Pathol 2016;40:244–252.
17 Webber C, Gospodarowicz M, Sobin LH, Wittekind C, Greene FL, Mason MD, Compton C, Brierley J, Groome PA: Improving the TNM classification: findings from a 10-year continuous literature review. Int J Cancer 2014;135:371–378.
18 Park SY, Shin SJ, Jung DC, Cho NH, Choi YD, Rha KH, Hong SJ, Oh YT: PI-RADS version 2: quantitative analysis aids reliable interpretation of diffusion-weighted imaging for prostate cancer. Eur Radiol 2017;27:2776–2783.
19 Viera AJ, Garrett JM: Understanding interobserver agreement: the kappa statistic. Fam Med 2005;37:360–363.
20 D'Amico AV, Whittington R, Malkowicz SB, Fondurulia J, Chen MH, Tomaszewski JE, Wein A: The combination of preoperative prostate specific antigen and postoperative pathological findings to predict prostate specific antigen outcome in clinically localized prostate cancer. J Urol 1998;160:2096–2101.
21 Barth BK, Cornelius A, Nanz D, Eberli D, Donati OF: Diffusion-weighted imaging of the prostate: image quality and geometric distortion of readout-segmented versus selective-excitation accelerated acquisitions. Invest Radiol 2015;50:785–791.
22 Beyersdorff D, Darsow U, Stephan C, Schnorr D, Loening S, Taupitz M: MRI of prostate cancer using three different coil systems: image quality, tumor detection, and staging. Rofo 2003;175:799–805.
23 Futterer JJ, Engelbrecht MR, Jager GJ, Hartman RP, King BF, Hulsbergen-Van de Kaa CA, Witjes JA, Barentsz JO: Prostate cancer: comparison of local staging accuracy of pelvic phased-array coil alone versus integrated endorectal-pelvic phased-array coils. Local staging accuracy of prostate cancer using endorectal coil MR imaging. Eur Radiol 2007;17:1055–1065.
24 Rosenkrantz AB, Deng FM, Kim S, Lim RP, Hindman N, Mussi TC, Spieler B, Oaks J, Babb JS, Melamed J, Taneja SS: Prostate cancer: multiparametric MRI for index lesion localization--a multiple-reader study. AJR Am J Roentgenol 2012;199:830–837.
25 Futterer JJ, Briganti A, De Visschere P, Emberton M, Giannarini G, Kirkham A, Taneja SS, Thoeny H, Villeirs G, Villers A: Can clinically significant prostate cancer be detected with multiparametric magnetic resonance imaging? A systematic review of the literature. Eur Urol 2015;68:1045–1053.
26 Jordan EJ, Fiske C, Zagoria RJ, Westphalen AC: Evaluating the performance of PI-RADS v2 in the non-academic setting. Abdom Radiol (NY) 2017;42:2725–2731.
27 Liddell H, Jyoti R, Haxhimolla HZ: mp-MRI prostate characterised PIRADS 3 lesions are associated with a low risk of clinically significant prostate cancer - a retrospective review of 92 biopsied PIRADS 3 lesions. Curr Urol 2015;8:96–100.
28 Srirangam V, Rai BP, Abroaf A, Agarwal S, Tadtayev S, Foley C, Lane T, Adshead J, Vasdev N: Atypical small acinar proliferation and high grade prostatic intraepithelial neoplasia: should we be concerned? An observational cohort study with a minimum follow-up of 3 years. Curr Urol 2017;10:199–205.
29 Barth BK, De Visschere PJL, Cornelius A, Nicolau C, Vargas HA, Eberli D, Donati OF: Detection of clinically significant prostate cancer: short dual-pulse sequence versus standard multiparametric MR imaging-a multireader study. Radiology 2017;284:725–736.
30 Hoeks CM, Schouten MG, Bomers JG, Hoogendoorn SP, Hulsbergen-van de Kaa CA, Hambrock T, Vergunst H, Sedelaar JP, Futterer JJ, Barentsz JO: Three-Tesla magnetic resonance-guided prostate biopsy in men with increased prostate-specific antigen and repeated, negative, random, systematic, transrectal ultrasound biopsies: detection of clinically significant prostate cancers. Eur Urol 2012;62:902–909.
31 Kasivisvanathan V, Dufour R, Moore CM, Ahmed HU, Abd-Alazeez M, Charman SC, Freeman A, Allen C, Kirkham A, van der Meulen J, Emberton M: Transperineal magnetic resonance image targeted prostate biopsy versus transperineal template prostate biopsy in the detection of clinically significant prostate cancer. J Urol 2013;189:860–866.
32 Rais-Bahrami S, Siddiqui MM, Turkbey B, Stamatakis L, Logan J, Hoang AN, Walton-Diaz A, Vourganti S, Truong H, Kruecker J, Merino MJ, Wood BJ, Choyke PL, Pinto PA: Utility of multiparametric magnetic resonance imaging suspicion levels for detecting prostate cancer. J Urol 2013;190:1721–1727.
33 Thompson JE, Moses D, Shnier R, Brenner P, Delprado W, Ponsky L, Pulbrook M, Bohm M, Haynes AM, Hayen A, Stricker PD: Multiparametric magnetic resonance imaging guided diagnostic biopsy detects significant prostate cancer and could reduce unnecessary biopsies and over detection: a prospective study. J Urol 2014;192:67–74.
34 Donati OF, Jung SI, Vargas HA, Gultekin DH, Zheng J, Moskowitz CS, Hricak H, Zelefsky MJ, Akin O: Multiparametric prostate MR imaging with T2-weighted, diffusion-weighted, and dynamic contrast-enhanced sequences: are all pulse sequences necessary to detect locally recurrent prostate cancer after radiation therapy? Radiology 2013;268:440–450.
35 Lin WC, Muglia VF, Silva GE, Chodraui Filho S, Reis RB, Westphalen AC: Multiparametric MRI of the prostate: diagnostic performance and interreader agreement of two scoring systems. Br J Radiol 2016;89:20151056.
36 Park SY, Jung DC, Oh YT, Cho NH, Choi YD, Rha KH, Hong SJ, Han K: Prostate cancer: PI-RADS Version 2 helps preoperatively predict clinically significant cancers. Radiology 2016;280:108–116.
37 Rosenkrantz AB, Lim RP, Haghighi M, Somberg MB, Babb JS, Taneja SS: Comparison of interreader reproducibility of the prostate imaging reporting and data system and likert scales for evaluation of multiparametric prostate MRI. AJR Am J Roentgenol 2013;201:W612–618.